Heptacoordinate Rhenium(III)-Bis(terpyridine) Complexes: Syntheses, Characterizations, and Crystal Structures of $[Re(terpyridine)_2X]^{2+}$ (X = OH, Cl, NCS). Substitution Kinetics of $[Re(terpyridine)_2OH]^{2+}$

Jochen Rall,[1] Franz Weingart,[2] Douglas M. Ho,[3] Mary Jane Heeg,*[4] Francesco Tisato,[5] and Edward Deutsch*[6]

Biomedical Chemistry Research Center, Department of Chemistry, University of Cincinnati, Cincinnati, Ohio 45221-0172, and Department of Chemistry, Wayne State University, Detroit, Michigan 48202-3929

Received January 14, 1994®

The 7-coordinated Re(III) complex $[Re(terpy)_2OH]^{2+}$, where terpy = 2,2':6',6''- terpyridine, has been synthesized and characterized. Preparation of this complex from $[Re^{V}O_2(pyridine)_4]^{+}$ occurs via a reduction/substitution route utilizing 2 molar equiv of terpyridine. The concomitant production of ReO_4^- implies the presence of a disproportionation component in the preparative reaction. Replacement of the coordinated hydroxo ligand by Cl^- or NCS^- to generate respectively the $[Re(terpy)_2Cl]^{2+}$ or $[Re(terpy)_2NCS]^{2+}$ complex proceeds much more rapidly at low pH. The X-ray crystal structure analyses of all three novel complexes are reported: $[Re(terpy)_2OH](PF_6)_2 \cdot H_2O$ crystallizes in the triclinic space group $P\bar{1}$ with $a = 9.099(1)$ Å, $b = 10.781(2)$ Å, $c = 17.438(3)$ Å, $\alpha = 82.87(1)°$, $\beta = 88.85(1)°$, $\gamma = 86.83(1)°$, $V = 1694.6(4)$ Å^3, and $Z = 2$. $[Re(terpy)_2Cl](PF_6)_2$ crystallizes in the monoclinic space group $P2_1/c$ with $a = 9.257(2)$ Å, $b = 19.597(5)$ Å, $c = 17.899(5)$ Å, $\beta = 94.85(2)°$, $V = 3235(1)$ Å^3, and $Z = 4$. $[Re(terpy)_2NCS](SCN)_2 \cdot {}^1/_2H_2O$ crystallizes in the triclinic space group $P\bar{1}$ with $a = 10.067(4)$ Å, $b = 11.121(2)$ Å, $c = 15.133(7)$ Å, $\alpha = 89.63(3)°$, $\beta = 80.04(4)°$, $\gamma = 75.46(3)°$, $V = 1614(1)$ Å^3, and $Z = 2$. The solution structure is fully determined by proton NMR and is shown to be similar to that in the solid state with two equivalent, but asymmetric, terpy ligands. In addition, the $[Re(terpy)_2X]^{2+}$ complexes are characterized by elemental analysis, UV-vis, IR, and mass spectroscopy, and/or thin-layer chromatography. A preliminary kinetic study of the substitution reaction of $[Re(terpy)_2OH]^{2+}$ to yield $[Re(terpy)_2NCS]^{2+}$ indicates that the hydroxy complex is involved in a rapid protonation equilibrium to yield a reactive species which then reacts with SCN^- in a rate determining step. Derived equilibrium and rate constants at 25 °C and $\mu = 1.00$ M are $pK_a = 1.4(8)$ and $k = 45(4)$ M^{-1} s^{-1}. The reverse reaction rate is insignificant under the conditions utilized.

Introduction

Terpyridine complexes of many transition metals have been synthesized and characterized. In most cases these complexes exhibit octahedral coordination geometry, independent of whether one or two terpyridine ligands are incorporated. For example, five bis(terpyridine) complexes of first-row transition metals (from Fe(II) to Cu(II) and Cr(III) and Co(III)) have been structurally characterized and all are 6-coordinate.[7] We recently reported the first tridentate terpyridine complex of the larger third-row metal rhenium; this complex possesses the formula $[ReO(terpy)(SC_6H_4CH_3)_2]^{+}$ and exhibits 6-coordinate, approximately octahedral geometry in spite of containing the tightly bound $(Re^{V}{=}O)^{3+}$ core.[8]

We now report this companion study, which describes surprisingly stable 7-coordinate bis(terpyridine) complexes of Re(III). These 7-coordinate Re(III)-terpyridine species, glimpsed as reaction byproducts in our earlier work,[8] are herein fully characterized. They are members of the class of complexes $[Re(terpy)_2X]^{2+}$ and are the first 7-coordinate bis(terpyridine) complexes to be prepared. The heavier transition metals often exhibit expanded coordination shells, and the question thus arises as to what constitutes the basis for observed coordination number. Both Re(III) and Tc(III) can be either 6-coordinate or 7-coordinate. 6-Coordination seems to be normal for ionic complexes; 7-coordination with Re(III) or Tc(III) (d^4) creates an 18-electron filled shell which shows a preference for covalent (π-back-bonding) ligands. The structural studies reported herein show that the observed distorted capped trigonal prismatic coordination geometry is closely related to ordinary bis(terpyridine) octahedral geometry, and upon ejection of the seventh ligand, only a small facial twist in the ligands is required to restore octahedral geometry. This implies that in solution an equilibrium between 6- and 7-coordinate species may occur and that a low-energy intermediate in the exchange of the X ligand may be the 6-coordinate bis(terpyridine) complex. In response to these considerations, a kinetic study of the substitution reaction producing $[Re(terpy)_2NCS]^{2+}$ from $[Re(terpy)_2OH]^{2+}$ was undertaken. The kinetic results are most reasonably interpreted by invoking a rapid 7-coordinate/6-coordinate equilibrium prior to the rate-determining step.

Acronyms and Abbreviations. The following acronyms and abbreviations are used in this article: BES = *N*,*N*-bis(2-hydroxyethyl)-2-aminoethanesulfonic acid; 2D-COSY = two-

® Abstract published in *Advance ACS Abstracts*, June 1, 1994.

(1) Current address: Institut fuer Anorganische Chemie, Universitaet Stuttgart, 70550 Stuttgart, Germany.
(2) Current address: Schuetzenstrasse 18, D-70190 Stuttgart, Germany.
(3) Current address: Department of Chemistry, Princeton University, Princeton, NJ 08544.
(4) Wayne State University.
(5) On leave from the Consiglio Nazionale delle Ricerche, Instituto di Chimica e Technologia Inorganiche e dei Materiali Avanzati, Corso Stati Uniti 4, 35020 Padova, Italy.
(6) Current address: Mallinckrodt Medical, Inc., 675 McDonnell Blvd., P. O. Box 5840, St. Louis, MO 63134.
(7) (a) Wickramasinghe, W. A.; Bird, P. H.; Serpone, N. *Inorg. Chem.* **1982**, *21*, 2694-8. (b) Baker, A. T.; Goodwin, H. A. *Aust. J. Chem.* **1985**, *38*, 207-14. (c) Figgis, B. N.; Kucharski, E. S.; White, A. H. *Aust. J. Chem.* **1983**, *36*, 1527-35, 1537-61, 1563-71. (d) Arriortua, M. I.; Rojo, T.; Amigo, J. M.; Germain, G.; Declercq, J. P. *Bull. Soc. Chim. Belg.* **1982**, *91*, 337-8; *Acta Crystallogr.* **1982**, *B38*, 1323-4.
(8) (a) Chang, L.; Rall, J.; Tisato, F.; Deutsch, E.; Heeg, M. J. *Inorg. Chim. Acta* **1993**, *205*, 35-44. (b) The structure of $[Re^{I}(terpy)(CO)_3Cl]$ has also been published, but the terpy ligand is bound in a bidentate manner: Anderson, P. A.; Keene, F. R.; Horn, E.; Tiekink, E. R. T. *Appl. Organomet. Chem.* **1990**, *4*, 523-33.

0020-1669/94/1333-3442$04.50/0

dimensional homonuclear shift correlation; DMPE = 1,2-bis(dimethylphosphino)ethane; DPPE = 1,2-bis(diphenylphosphino)ethane; Et = ethyl; EXAFS = extended X-ray analysis of fine structure; FAB = fast atom bombardment; ^{1}H NMR = proton nuclear magnetic resonance; IR = infrared; MES = 2-morpholinoethanesulfonic acid; Ph = phenyl; py = pyridine; TAPS = *N*-(tris(hydroxymethyl)methyl)-3-aminopropanesulfonic acid; terpy = 2,2′:6′6″-terpyridine; TLC = thin-layer chromatography.

Experimental Section

Materials. All chemicals were of reagent grade unless otherwise noted. Ammonium perrhenate (99+%), lithium trifluoromethanesulfonate (97+%) and trifluoromethanesulfonic acid (98+%) were purchased from Aldrich. 2,2′:6′,6″-Terpyridine was obtained from G. F. Smith Chemicals. Lithium carbonate (ultrapure) and trifluoromethanesulfonic acid (100%) were obtained from Johnson Matthey Alfa Products. Pyridine and all solvents were supplied by Fisher and used without further purification. House distilled water was used except in the case of kinetic experiments, which were performed with water that had been purified by a Barnstedt NANO-pure system with four filters and ion exchange cartridges. The starting materials $[ReOCl_2(OEt)(PPh_3)]$, $[ReO_2(py)_4]CF_3SO_3\cdot 2H_2O$, and $[ReO_2(py)_4]Cl\cdot 2H_2O$ were prepared as reported.[8a] TLC plastic sheets (silica gel 60 F_{254}, layer thickness 0.2 mm) were obtained from Merck. The mobile phase used in TLC was HPLC-grade acetonitrile/0.1 M lithium trifluoromethanesulfonate, except for the $[Re(terpy)_2Cl]^{2+}$ experiment, wherein the mobile phase was also saturated with NH_4Cl to prevent decomposition of the chloro complex.

Synthesis of $[Re(terpy)_2OH](ReO_4)_2$ and $[Re(terpy)_2OH](PF_6)_2$. To prepare salts of the hydroxobis(2,2′:6′,6″-terpyridine)rhenium(III) cation, 1.21 g of $[ReO_2(py)_4]CF_3SO_3\cdot 2H_2O$ (1.68 mmol) was dissolved in 100 mL of a 2:5 ethanol/water mixture. Terpyridine (0.84 g, 3.6 mmol) was added, and the reaction mixture was refluxed for 18 h. The resulting dark red solution was extracted three times with diethyl ether to remove excess terpyridine, pyridine, and most of the ethanol. After the solution had been stored in a refrigerator for 3 days, crystals or precipitate formed; this solid was removed by filtration, washed with a small amount of ice-cold water and then with diethyl ether, and dried. The complex was recrystallized by slow evaporation of an acetonitrile/toluene solution at room temperature. At this step, the product contained both perrhenate and triflate as counterions. The perrhenate salt was less soluble and easily precipitated from the reaction mixture. Addition of aqueous NH_4ReO_4 to the still dark red mother liquor produced further $[Re(terpy)_2OH](ReO_4)_2$ material. Yield: 20%. The bis(hexafluorophosphate) derivative was prepared by adding concentrated aqueous NH_4PF_6 after the extraction procedure. Crystals suitable for X-ray analysis were collected by slowly evaporating over a period of several days a solution of pure $[Re(terpy)_2OH](PF_6)_2$ dissolved in a 75:25 water/ethanol mixture.

Anal. Calcd for $[Re(terpy)_2OH](PF_6)_2\cdot H_2O$ ($RePF_{12}O_2N_6C_{30}H_{25}$): C, 36.86; H, 2.58; N, 8.59; Re, 19.05. Found: C, 36.68; H, 2.59; N, 8.54; Re, 19.04.

Data for $[Re(terpy)_2OH](ReO_4)_2\cdot H_2O$ are as follows. UV–vis (CH_3CN): λ_{max} (nm) = 520, 474 sh, 361, 325, 290. IR (cm^{-1}): 1603 (m), 1451 (m), 1384 (s), 1279 (w), 1016 (w), 911 (vs), 866 (w), 768 (m). FAB MS (*m/z*), positive mode: 670 at 52% intensity (M^+), 654 at 52% intensity ($M^+ - O$), 437 at 100% intensity (M^+ – terpy). TLC R_f: 0.11.

Synthesis of $[Re(terpy)_2Cl](Cl)_2$, $[Re(terpy)_2Cl](ReO_4)_2$, and $[Re(terpy)_2Cl](PF_6)_2$. $[ReO_2(py)_4]CF_3SO_3\cdot 2H_2O$ (2.1 g, 3.46 mmol) was dissolved in 80 mL of a 1:1 ethanol/water mixture. Then terpyridine (2.11 g, 9 mmol) and NH_4Cl (4 g, 75 mmol) were added and the reaction mixture was refluxed for 18 h. The resulting dark red solution was extracted three times with ethyl ether to remove excess terpyridine, pyridine, and most of the ethanol. Upon storage in the refrigerator, this solution yielded crystals or a fine precipitate after a few days. The crude product was recrystallized by slow evaporation of an acetonitrile/toluene solution at room temperature. Perrhenate and chloride were both present as counterions when the final product was recovered. The bis(hexafluorophosphate) derivative was isolated by adding a concentrated aqueous solution of NH_4PF_6 after the extraction procedure. $[Re(terpy)_2Cl]^{2+}$ was usually contaminated by a small amount of the $[Re(terpy)_2OH]^{2+}$ complex; therefore, no accurate percent yield can be given. To avoid this contamination, after the extraction process the solution was acidified with HCl and aqueous NH_4ReO_4 was added. After a few minutes a pale red precipitate of pure $[Re(terpy)_2Cl](ReO_4)_2$ formed in very low yield. Crystals suitable for X-ray analysis were grown as follows. A sample of $[Re(terpy)_2Cl](PF_6)_2$ contaminated with the hydroxo complex was dissolved in a 3:1 water/ethanol mixture. Upon slow evaporation over a period of several days, crystals of differing habits appeared. The chloro complex crystallized as small red-purple prisms which could be picked out of the sample and used for X-ray diffraction experiments.

Data for $[Re(terpy)_2Cl](Cl)_2$ are as follows. UV–vis (CH_3CN) λ_{max} (nm): 496, 325, 290. IR (cm^{-1}): 1608 (m), 1453 (m), 1386 (m), 1280 (w), 1252 (w), 1015 (w), 865 (w), 767 (m), 314 (m). FAB MS (*m/z*), positive mode: 689 at 76% intensity (M^+), 654 at 100% intensity (M^+ – Cl). TLC R_f: 0.34.

Synthesis of $[Re(terpy)_2NCS](CF_3SO_3)_2$ and $[Re(terpy)_2NCS](SCN)_2$. $[Re(terpy)_2OH](ReO_4)_2\cdot H_2O$ (150 mg, 0.13 mmol) was dissolved in 50 mL of acetonitrile. Three drops of a 7 M CF_3SO_3H solution and 50 mg of KSCN (0.5 mmol) dissolved in 10 mL of acetonitrile were added. The color changed immediately from purple to orange. Some white precipitate, presumably $KReO_4$, formed and was removed by filtration. The filtrate was layered over toluene and allowed to evaporate slowly at room temperature. Orange crystals were removed by filtration, washed with toluene and ether, and dried. At this point, the FAB MS (negative-ion mode) demonstrated that the anion was mostly $CF_3SO_3^-$, but SCN^- was also present. Yield: 99 mg, 65%. Crystals of $[Re(terpy)_2NCS](SCN)_2\cdot {}^1/_2H_2O$ suitable for X-ray analysis formed after several weeks in an aqueous solution containing 10^{-4} M $[Re(terpy)_2OH][ReO_4]_2\cdot H_2O$, 1 M KSCN, and 0.01 M CF_3SO_3H.

Data for $[Re(terpy)_2NCS](CF_3SO_3)_2$ are as follows. Vis (CH_3CN): λ_{max} = 476 nm. IR (cm^{-1}): 2362 (m), 2047 (s), 1603 (m), 1448 (m), 1384 (s), 1277 (w), 1261 (w), 1032 (w), 1016 (w), 786 (w), 766 (m), 719 (w), 668 (w), 645 (w), 519 (w), 465 (w). TLC R_f: 0.40.

Measurements. Elemental analyses were performed by Galbraith Laboratories, Knoxville, TN. IR spectra were recorded on a Perkin-Elmer 1600 Series FT-IR spectrometer on KBr pellets. Electronic absorption spectra were recorded on a Cary 210 spectrophotometer (Varian) at room temperature. Time-dependent absorbance measurements for the kinetic experiments were conducted at 600 nm on a Cary 118B spectrophotometer, connected to a Haake FK2 thermocirculator with a Neslab "U-cool" bath cooler. The temperature was measured with a thermistor probe inside a cell contained in the multiple-cell compartment and displayed on a Digitec 581C digital thermometer; this temperature was constant within 0.1 °C. FAB mass spectra were measured in the positive- or negative-ion mode on a VG 30–250 quadrapole Masslab instrument (VG Instruments Inc.) at the probe temperature using a glycerol or *m*-nitrobenzyl alcohol matrix. Xenon was used as the primary gas beam, and the ion gun was operated at 7 keV and 1 mA. Data were collected generally over the mass range 100–1000 Da at 0.7 s/scan. Proton NMR spectra were recorded at 250 MHz on a Bruker AC-250 spectrometer. The TLC characterizations were performed with the materials mentioned above. R_f values were very dependent on the concentration of $LiCF_3SO_3$.

Crystallography. Single-crystal X-ray diffraction experiments were performed on Nicolet R3 automated diffractometers with Mo Kα radiation and graphite monochromator at ambient temperature. $\theta/2\theta$ scans were used for data collection. The structures were refined with the programs of SHELX-76 and SHELXTL.[9a] Absorption corrections were made by empirical methods or by Gaussian intergration. All non-hydrogen atoms are described anisotropically. Neutral-atom scattering factors and corrections for anomalous dispersion were from ref 9b. Table 1 contains further experimental data.

Kinetic Reagents. All solutions were prepared with NANO-pure water (*vide supra*). Concentrations of stock solutions were determined by standard volumetric titrations, using 0.100 N NaOH for acids, 0.100 N HCl for bases, and 0.100 N $AgNO_3$ for SCN^- solutions. The ionic strength was adjusted by using a lithium trifluoromethanesulfonate solution prepared as follows. An 18.473-g sample (0.25 mol) of Ultrapure lithium carbonate was neutralized with *ca.* 7 M trifluoromethanesulfonic acid, and the resulting solution was heated. After a clear solution was obtained, it was diluted with NANO-pure water to 100 mL in a volumetric flask. The final CF_3SO_3Li solution was slightly acidic.

The concentration of H^+ was held constant through the use of appropriate buffers. If $[H^+]$ was greater than a 10-fold excess over $[[Re(terpy)_2OH]^{2+}]$, no buffer was necessary because $[H^+]$ was ap-

(9) (a) Sheldrick, G. M. *SHELX-76*. University Chemistry Laboratory, Cambridge, England, 1976. Sheldrick, G. M. *SHELXTL*. University of Göttingen, Göttingen, Germany, 1978. (b) *International Tables for X-ray Crystallography*; Kynoch: Birmingham, U.K., 1974; Vol. 4.

Table 1. Experimental Crystallographic Data[a]

	$[Re(terpy)_2OH](PF_6)_2 \cdot H_2O$	$[Re(terpy)_2Cl](PF_6)_2$	$[Re(terpy)_2NCS](SCN)_2 \cdot {}^1/_2H_2O$
formula	$ReP_2F_{12}O_2N_6C_{30}H_{25}$	$ReClP_2F_{12}N_6C_{30}H_{22}$	$ReS_3O_{0.5}N_9C_{33}H_{23}$
mol wt	977.70	978.13	836.00
space group	$P\bar{1}$	$P2_1/c$	$P\bar{1}$
cell dimens[b]			
a, Å	9.099(1)	9.257(2)	10.067(4)
b, Å	10.781(2)	19.597(5)	11.121(2)
c, Å	17.438(3)	17.899(5)	15.133(7)
α, deg	82.87(1)		89.63(3)
β, deg	88.85(1)	94.85(2)	80.04(4)
γ, deg	86.83(1)		75.46(3)
V, Å^3	1694.6(4)	3235(1)	1614(1)
Z	2	4	2
ρ(calc), g cm^{-3}	1.916	2.008	1.720
μ, cm^{-1}	38.29	40.88	40.41
transm coeff	0.894–0.619	0.615–0.546	0.660–0.304
R, R_w	0.029, 0.040	0.059, 0.054	0.044, 0.052

[a] T = 22 °C; λ = 0.710 73 Å; $R = (\sum||\Delta F|)/\sum|F_o|$; $R_w = [\sum w|\Delta F|^2)/\sum wF_o^2]^{1/2}$. [b] Lattice parameters from 25 high-angle reflections.

proximately constant during the reaction. In this case, the concentration of acid was adjusted with CF_3SO_3H and the final pH of the reaction mixture was measured. In the pH range 5.5–9.0, zwitterionic and sterically hindered amines were used as buffers. These "Good's buffers" are reported to be substantially non-nucleophilic and are considered to be noncoordinating.[10] The three noncoordinating "Good's buffers" used in this work are MES (pK_a = 6.1), BES (pK_a = 7.1) and TAPS (pK_a = 8.4). In the pH range 2.7–5.5, a number of buffers were tested (acetic acid, formic acid, phosphoric acid, and citric acid) and all were found to influence the observed reaction. The lack of readily available, water-soluble and noncoordinating buffers in this pH range prohibited meaningful kinetic experiments between pH 2.7 and 5.5.

Aqueous solutions of HNCS are not very stable,[11] but since the reported pK_a values of HNCS are always smaller than 1, and generally between −1.5 and −2.0,[12] no precautions for SCN^- decomposition were taken into account in these experiments. However, care was taken not to add thiocyanate to very acidic solutions. A stock solution of 10^{-3} M $[Re(terpy)_2OH](ReO_4)_2$ was prepared and used throughout the kinetic measurements.

Kinetic Procedure. Reactions were run with an initial concentration of 1.66×10^{-4} M in $[Re(terpy)_2OH](ReO_4)_2$, using a large excess of thiocyanate (0.002 M to 0.8 M) at 25 °C in a thermostated sample compartment. CF_3SO_3Li was added to maintain an ionic strength of 1.00 M. The pH of the solution was adjusted with LiOH if buffers were used, and the final pH value was measured in the reaction solution. Typically, a solution of KSCN, buffer or acid, and CF_3SO_3Li was prepared at 25 °C and adjusted with LiOH if necessary to obtain the desired pH. An aliquot of this solution was pipetted into a thermostated spectrophotometric cell and the reaction started upon addition of an aliquot of $[Re(terpy)_2OH](ReO_4)_2$. Reliable absorbance values could be obtained about 5–7 s after mixing. All kinetic experiments were monitored at 600 nm. Absorption and extinction data for the complexes involved are given in Table 2. Plots of $-\ln(A_t - A_\infty)$ vs time were linear over *ca.* 4 half-lives.

Absorbance data from the Cary 118B spectrophotometer were recorded digitally. Nonlinear regression was performed on a personal computer with a BASIC program based on a method described by Wentworth.[13] Activation parameters were obtained from a nonlinear least-squares fit of the Eyring equation with $\Delta H^\ddagger$ and $\Delta S^\ddagger$ as adjustable parameters. The temperature was varied over 10 °C increments throughout the range 15–65 °C for these studies.

Results

Synthesis. The terpyridine–Re(III) 7-coordinate complex $[Re(terpy)_2OH]^{2+}$ can be synthesized by refluxing $[Re^VO_2(py)_4]CF_3SO_3$ with terpyridine in an ethanol/water mixture for 18 h. After extraction of excess reagents, a solid precipitate is formed upon cooling the reaction mixture. Any source of chloride ions in the preparation (*e.g.* the use of the starting material $[ReO_2(py)_4]Cl$ or the addition of NH_4Cl during the procedure) results in a mixture of $[Re(terpy)_2Cl]^{2+}$ and $[Re(terpy)_2OH]^{2+}$ products. Pure $[Re(terpy)_2Cl]^{2+}$ could only be produced from an acid (HCl)/aqueous perrhenate solution. The isothiocyanato complex $[Re(terpy)_2NCS]^{2+}$ can be prepared from $[Re(terpy)_2OH]^{2+}$ in acetonitrile and an excess of KSCN and CF_3SO_3H.

Table 2. Visible–UV Spectroscopic Data[a]

complex	λ_{max}, nm (ϵ, M^{-1} cm^{-1})	ϵ_{600nm}, M^{-1} cm^{-1} [b]
$[Re(terpy)_2OH]^{2+}$ [c]	512 (13 110)	4150
	466 sh (10 460)	
	354 (4520)	
	327 (33 810)	
	292 (36 110)	
	203 (90 560)	
$[Re(terpy)_2OH_2]^{3+}$ [d]	486 (9780),	1450
	328 (30 790)	
	288 (34 660)	
	224 (41 660)	
$[Re(terpy)_2NCS]^{2+}$ [e]	478 (12 170)	1110

[a] In water. [b] The wavelength at which all kinetic experiments were monitored. [c] 8.28×10^{-5} M $[Re(terpy)_2OH]^{2+}$; spectrum measured over λ = 200–700 nm. [d] 8.28×10^{-5} M $[Re(terpy)_2OH]^{2+}$ and 0.4 M CF_3SO_3H; spectrum measured over λ = 200–700 nm. [e] 8.28×10^{-5} M $[Re(terpy)_2OH]^{2+}$ and 1 M KSCN at pH 2 with CF_3SO_3H; spectrum measured over λ = 350–700 nm due to strong absorption of KSCN in the UV region.

Crystallography. The three complexes $[Re(terpy)_2OH](PF_6)_2 \cdot H_2O$, $[Re(terpy)_2Cl](PF_6)_2$, and $[Re(terpy)_2NCS](SCN)_2 \cdot {}^1/_2H_2O$ have been examined by single-crystal X-ray analyses. Molecular diagrams of the cations are presented in Figures 1–3 along with the atomic labeling schemes which are purposely similar. Fractional atomic coordinates and selected bond lengths and angles are listed separately for each complex in Tables 3–8.

The geometries of the three cations are closely similar. The central Re atom is 7-coordinate, bonding to three nitrogen donors from each of two terpy ligands and having a seventh bond to either hydroxide, chloride, or thiocyanate-*N*. The overall arrangement of the donor atoms around rhenium is distorted from an ideal capped trigonal prism, which is one of the three commonly observed geometries for 7-coordinate complexes (*viz.* capped octahedron, capped trigonal prism, and pentagonal bipyramid).[14] In these structures, the quadrilateral face is occupied by one central and one outer nitrogen atom of each of the two terpy ligands (N2, N3, N4, N6). The edge positions are comprised of

(10) (a) Good, N. E.; Winget, G. D.; Winter, W.; Connolly, T. N.; Izawa, S.; Singh, R. M. M. *Biochemistry* **1966**, *5*, 467. (b) Wilkins, R. G. *The Study of Kinetics and Mechanism of Reactions of Transition Metal Complexes*; Allyn and Bacon: Boston, 1974.
(11) *Gmelin Handbook der Anorganischen Chemie*, 8th ed.; Springer-Verlag: Berlin, 1978; Kohlenstoff Teil D6, pp 22.
(12) *Gmelin Handbook der Anorganischen Chemie*, 8th ed.; Springer-Verlag: Berlin, 1978; Kohlenstoff Teil D6, p 21, 25.
(13) Wentworth, W. E. *J. Chem. Educ.* **1965**, *42*, 96–103, 162–7.
(14) (a) Muetterties, E. L.; Guggenberger, L. J. *J. Am. Chem. Soc.* **1974**, *96*, 1748–56. (b) Muetterties, E. L.; Guggenberger, L. J. *J. Am. Chem. Soc.* **1977**, *99*, 3893. (c) Kouba, J. K.; Wreford, S. S. *Inorg. Chem.* **1976**, *15*, 1463–65. (d) Drew, M. G. B. *Prog. Inorg. Chem.* **1977**, *23*, 67–210.

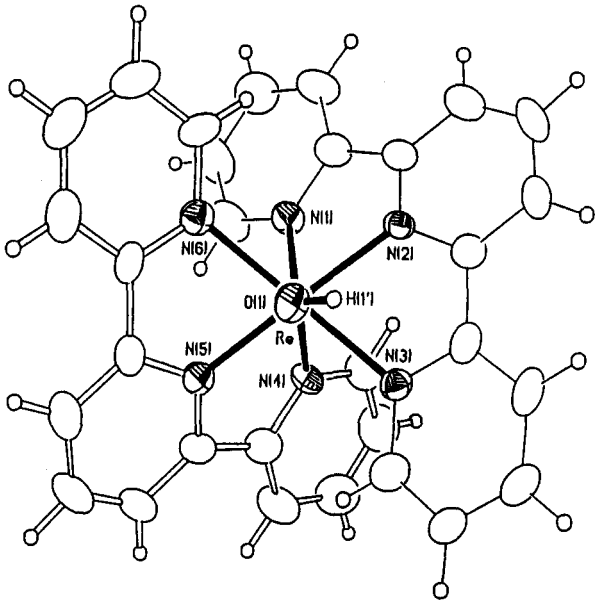

Figure 1. Molecular diagram of $[Re(terpy)_2OH]^{2+}$ illustrating the geometry and assigned labeling.

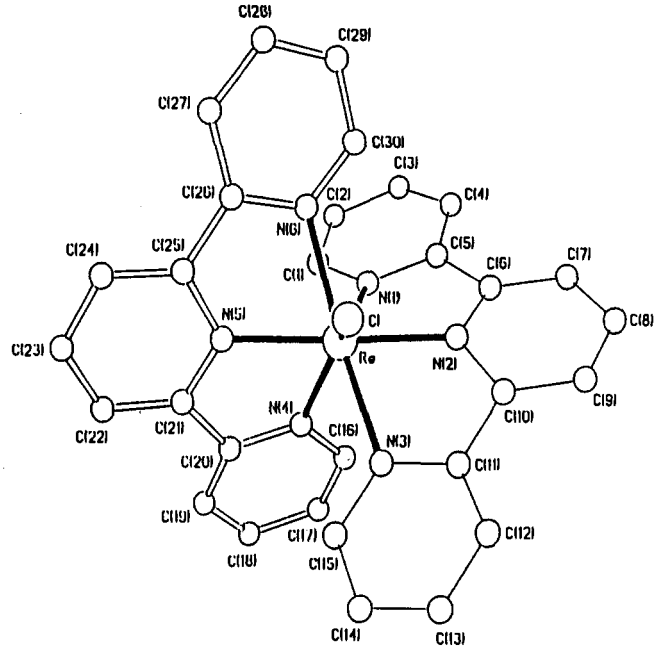

Figure 2. Molecular diagram of $[Re(terpy)_2Cl]^{2+}$ illustrating the geometry and assigned labeling.

the remaining outer nitrogen atom from each terpy ligand (N1 and N4). The one non-terpy donor ligand in each complex (OH, Cl, or NCS) occupies a capping site.

The three terpyridine nitrogen atoms are asymmetrically bound to the Re atom, and thus individual types of Re–N bonds vary in length. The shortest Re–N(terpy) distance involves the central terpy nitrogen atom located in the axial positions of the coordination polyhedon and averages in these structures 2.06(1) Å. Regarding the outer terpy nitrogen atoms, each terpy ligand has one shorter and one longer bond to rhenium. The longer Re–N distance is to the outer terpy nitrogen atom nearest the seventh (monodentate) ligand in the quadrilateral face; the average is 2.16(1) Å. Shorter Re–N distances are observed for the remaining nitrogen atoms in the edge positions (2.10(2) Å). The terpy ligands exhibit a moderate amount of ring twisting between the pyridine ring components (8–18°). For the monodentate ligands, Re–OH = 1.969(5) Å, Re–Cl = 2.281(5) Å, and Re–NCS = 2.046(9) Å. The NCS^- ligand is linear (179.3(9)°).

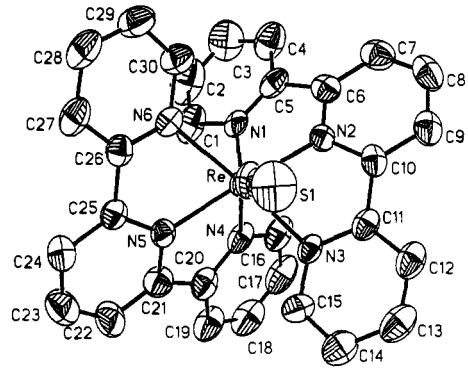

Figure 3. Molecular diagram of $[Re(terpy)_2NCS]^{2+}$ illustrating the geometry and assigned labeling. The atoms N7 and C31 are eclipsed by S1 and are not labeled.

Table 3. Fractional Atomic Coordinates for $[Re(terpy)_2OH](PF_6)_2 \cdot H_2O$

atom	x	y	z
Re	0.0813(1)	0.2518(1)	0.2287(1)
O1	–0.0808(5)	0.3691(5)	0.1888(3)
N1	0.3123(6)	0.2264(5)	0.2214(3)
N2	0.1671(6)	0.3837(5)	0.2895(3)
N3	–0.0586(6)	0.2646(5)	0.3290(3)
N4	0.1210(6)	0.0761(5)	0.2962(3)
N5	–0.0087(6)	0.1187(5)	0.1712(3)
N6	0.1306(6)	0.3034(5)	0.1076(3)
C1	0.3793(8)	0.1356(7)	0.1835(5)
C2	0.5231(9)	0.1414(9)	0.1582(6)
C3	0.6041(9)	0.2403(9)	0.1736(6)
C4	0.5420(8)	0.3312(8)	0.2155(5)
C5	0.3937(7)	0.3232(7)	0.2376(4)
C6	0.3107(8)	0.4093(6)	0.2812(4)
C7	0.3652(9)	0.5033(7)	0.3175(5)
C8	0.2752(10)	0.5699(7)	0.3630(5)
C9	0.1343(9)	0.5330(7)	0.3777(4)
C10	0.0816(8)	0.4382(6)	0.3421(4)
C11	–0.0502(8)	0.3734(6)	0.3611(4)
C12	–0.1649(9)	0.4124(7)	0.4090(4)
C13	–0.2831(8)	0.3397(7)	0.4263(5)
C14	–0.2857(8)	0.2265(7)	0.3952(4)
C15	–0.1733(8)	0.1930(7)	0.3477(4)
C16	0.1980(9)	0.0634(7)	0.3621(5)
C17	0.1927(10)	–0.0408(8)	0.4157(5)
C18	0.1055(11)	–0.1363(8)	0.4016(6)
C19	0.0308(10)	–0.1274(7)	0.3329(5)
C20	0.0410(8)	–0.0205(6)	0.2815(4)
C21	–0.0330(8)	0.0012(6)	0.2068(4)
C22	–0.1131(8)	–0.0785(7)	0.1715(5)
C23	–0.1629(8)	–0.0432(7)	0.0986(5)
C24	–0.1206(8)	0.0672(7)	0.0587(5)
C25	–0.0383(7)	0.1468(7)	0.0946(4)
C26	0.0365(7)	0.2556(6)	0.0591(4)
C27	0.0313(9)	0.3041(7)	–0.0177(4)
C28	0.1170(10)	0.3965(8)	–0.0470(5)
C29	0.2111(9)	0.4428(7)	0.0012(5)
C30	0.2138(8)	0.3966(7)	0.0790(5)
P1	–0.3356(2)	0.7653(2)	0.4462(1)
F1	–0.2873(11)	0.7358(9)	0.3661(5)
F2	–0.3944(8)	0.6245(7)	0.4633(6)
F3	–0.1813(8)	0.7127(8)	0.4720(6)
F4	–0.2799(9)	0.8967(6)	0.4302(6)
F5	–0.4974(8)	0.8042(9)	0.4220(6)
F6	–0.3837(10)	0.7803(10)	0.5309(5)
P2	–0.6003(3)	0.7593(3)	0.1165(2)
F7	–0.6491(9)	0.7266(7)	0.0381(5)
F8	–0.7002(18)	0.8801(9)	0.1070(7)
F9	–0.4697(17)	0.8135(18)	0.0894(11)
F10	–0.5245(14)	0.6286(9)	0.1364(7)
F11	–0.7360(16)	0.6924(16)	0.1515(8)
F12	–0.5702(17)	0.7885(11)	0.2005(7)
O2	–0.2554(10)	0.5975(8)	0.2383(6)

Characterization. In addition to the single crystal X-ray structural determinations, the terpy–Re(III) complexes reported herein are characterized by (i) elemental analyses for the

Table 4. Selected Bond Lengths (Å) and Angles (deg) for $[Re(terpy)_2OH](PF_6)_2 \cdot H_2O$

Re–O1	1.969(5)	N3–C15	1.344(9)
Re–N1	2.108(5)	N4–C16	1.346(9)
Re–N2	2.070(5)	N4–C20	1.356(9)
Re–N3	2.155(5)	N5–C21	1.367(9)
Re–N4	2.119(5)	N5–C25	1.360(9)
Re–N5	2.063(5)	N6–C26	1.379(9)
Re–N6	2.161(6)	N6–C30	1.332(9)
N1–C1	1.358(9)	C5–C6	1.44(1)
N1–C5	1.373(9)	C10–C11	1.43(1)
N2–C6	1.352(9)	C20–C21	1.47(1)
N2–C10	1.359(9)	C25–C26	1.45(1)
N3–C11	1.368(8)		
N1–Re–O1	140.6(2)	N6–Re–N2	107.7(2)
N2–Re–O1	92.1(2)	N6–Re–N3	150.8(2)
N2–Re–N1	73.3(2)	N6–Re–N4	128.3(2)
N3–Re–O1	76.9(2)	N6–Re–N5	74.0(2)
N3–Re–N1	129.4(2)	C1–N1–Re	122.0(4)
N3–Re–N2	73.2(2)	C5–N1–Re	117.3(4)
N4–Re–O1	141.4(2)	C6–N2–Re	120.3(5)
N4–Re–N1	77.8(2)	C10–N2–Re	119.9(4)
N4–Re–N2	106.3(2)	C11–N3–Re	114.4(4)
N4–Re–N3	76.5(2)	C15–N3–Re	124.3(5)
N5–Re–O1	87.8(2)	C16–N4–Re	122.3(4)
N5–Re–N1	107.9(2)	C20–N4–Re	118.0(4)
N5–Re–N2	178.2(2)	C21–N5–Re	121.9(5)
N5–Re–N3	105.0(2)	C25–N5–Re	119.0(5)
N5–Re–N4	72.8(2)	C26–N6–Re	113.4(4)
N6–Re–O1	73.9(2)	C30–N6–Re	125.3(5)
N6–Re–N1	76.1(2)		

prototypical complex $[Re(terpy)_2OH](PF_6)_2 \cdot H_2O$, the results of which are in good agreement with the proposed formulation, (ii) IR spectroscopy, (iii) FAB mass spectrometry, and/or (iv) thin-layer chromatography. The results obtained from applying these techniques are given in the Experimental Section.

The sensitivity of FAB mass spectroscopy is known to be low for 2+ cationic species; the monopositive fragments observed in these FAB MS analyses presumably result from Re(II) complexes generated during the analysis. Some FAB mass spectral peaks quoted herein occur in pairs which differ by two mass units representative of the $^{187}Re/^{185}Re$ isotopic ratio. For convenience, only the higher of the two peaks is listed. Positive-ion mode spectra show parent peaks at *m/z* 670 for $[Re^{II}(terpy)_2OH]^+$ and *m/z* 689 for $[Re^{II}(terpy)_2Cl]^+$. Several fragment ions corresponding to losses of oxygen and a terpy ligand are also observed for $[Re(terpy)_2OH]^{2+}$. In addition to the parent peak, the $[Re(terpy)_2Cl]^{2+}$ spectrum shows only one other assignable peak at *m/z* 654 corresponding to $[Re^{I}(terpy)_2]^+$. No satisfactory spectra were obtained for the $[Re(terpy)_2NCS]^{2+}$ complex. When crude samples of the reaction products were examined under negative-ion mode, the FAB mass spectra of $[Re(terpy)_2OH]^{2+}$ contained a major peak at *m/z* 250, consistent with the presence of perrhenate anion. Similarly, the IR spectrum of $[Re(terpy)_2OH](ReO_4)_2$ shows a very strong band around 910 cm^{-1} due to the stretching vibration of the Re=O group in the perrhenate anion. The IR spectrum of $[Re(terpy)_2NCS](CF_3SO_3)_2$ shows typical bonds associated with the coordinated NCS^- group at 2047, 786, and 465 cm^{-1}.

Thin-layer chromatography was used both to monitor the purity of the samples and to characterize the complexes as a function of their different lipophilicities arising from the nature of the seventh, monodentate, ligand X. On silica gel sheets in acetonitrile solutions containing 0.1 M CF_3SO_3Li, $[Re(terpy)_2NCS]^{2+}$ has the largest R_f value (~0.40) and $[Re(terpy)_2OH]^{2+}$ the smallest R_f value (~0.11).

Electronic Spectra. $[Re(terpy)_2X]^{2+}$ (X = OH, Cl, NCS) complexes all exhibit similar, characteristic, and well-defined absorption bands in the visible and UV regions. The visible spectra in acetonitrile are dominated by an intense absorption band around 500 nm with an extinction coefficient greater than 10^3 M^{-1} cm^{-1}.

Table 5. Fractional Atomic Coordinates for $[Re(terpy)_2C\ell](PF_6)_2$

atom	*x*	*y*	*z*
Re	0.1178(1)	0.1189(1)	0.2894(1)
Cℓ	–0.0457(5)	0.0356(3)	0.3110(3)
N1	0.3430(10)	0.1378(5)	0.2992(5)
N2	0.2058(10)	0.0561(5)	0.2144(5)
N3	–0.0305(10)	0.1173(6)	0.1903(5)
N4	0.1245(11)	0.2191(6)	0.2509(6)
N5	0.0282(10)	0.1781(6)	0.3690(6)
N6	0.1916(11)	0.0777(6)	0.3988(6)
Cℓ	0.4049(14)	0.1868(7)	0.3443(8)
C2	0.5499(15)	0.1882(8)	0.3631(9)
C3	0.6372(15)	0.1392(9)	0.3355(9)
C4	0.5789(14)	0.0892(8)	0.2889(8)
C5	0.4293(14)	0.0894(6)	0.2689(7)
C6	0.3497(14)	0.0437(7)	0.2177(7)
C7	0.4093(16)	–0.0057(7)	0.1727(8)
C8	0.3173(16)	–0.0408(7)	0.1215(7)
C9	0.1752(14)	–0.0240(7)	0.1129(7)
C10	0.1149(15)	0.0264(6)	0.1566(7)
C11	–0.0225(14)	0.0608(7)	0.1461(7)
C12	–0.1380(15)	0.0403(7)	0.0975(7)
C13	–0.2594(15)	0.0791(8)	0.0863(7)
C14	–0.2657(12)	0.1387(7)	0.1282(7)
C15	–0.1506(14)	0.1563(7)	0.1780(7)
C16	0.1959(14)	0.2381(7)	0.1908(8)
C17	0.1880(17)	0.3027(9)	0.1653(9)
C18	0.1087(19)	0.3535(9)	0.1983(9)
C19	0.0397(16)	0.3353(8)	0.2593(8)
C20	0.0473(13)	0.2682(7)	0.2841(7)
C21	–0.0113(13)	0.2444(8)	0.3516(8)
C22	–0.0940(14)	0.2808(8)	0.4009(9)
C23	–0.1249(17)	0.2506(11)	0.4681(9)
C24	–0.0644(15)	0.1886(9)	0.4882(8)
C25	0.0161(13)	0.1542(7)	0.4387(7)
C26	0.1040(13)	0.0966(7)	0.4547(6)
C27	0.1211(17)	0.0603(9)	0.5221(8)
C28	0.2219(18)	0.0076(9)	0.5324(10)
C29	0.3047(17)	–0.0079(8)	0.4748(10)
C30	0.2844(15)	0.0276(8)	0.4097(8)
P1	0.3180(4)	0.3548(2)	0.4839(2)
F1	0.3770(10)	0.4309(5)	0.4768(6)
F2	0.3619(12)	0.3582(6)	0.5712(5)
F3	0.1631(10)	0.3849(6)	0.4967(7)
F4	0.2795(14)	0.3513(7)	0.3989(6)
F5	0.4756(10)	0.3276(5)	0.4720(6)
F6	0.2603(11)	0.2790(5)	0.4907(6)
P2	0.3819(5)	–0.1605(3)	0.3208(3)
F7	0.2840(13)	–0.0977(6)	0.3015(8)
F8	0.4687(16)	–0.1225(9)	0.3822(11)
F9	0.2717(16)	–0.1852(9)	0.3731(8)
F10	0.2956(14)	–0.2001(7)	0.2548(8)
F11	0.4938(13)	–0.1385(8)	0.2658(11)
F12	0.4777(11)	–0.2248(6)	0.3382(7)

These maxima are listed in the Experimental Section. The energy and intensity of the visible band suggest that it is attributable to a M → L charge transfer transition. In water solutions, the maxima of the bands move to slightly shorter wavelengths. The UV regions show intense absorptions assigned to intraligand $\pi \rightarrow \pi^*$ transitions. The detailed electronic spectral data for $[Re(terpy)_2OH]^{2+}$, $[Re(terpy)_2OH_2]^{3+}$, and $[Re(terpy)_2NCS]^{2+}$ in water, relevant to the kinetics experiments, are listed in Table 2. Figure 4 contrasts the absorption spectra of $[Re(terpy)_2OH]^{2+}$ and $[Re(terpy)_2NCS]^{2+}$ in water.

Kinetics. The kinetics of NCS^- substitution onto $[Re(terpy)_2OH]^{2+}$ to yield $[Re(terpy)_2NCS]^{2+}$ were studied in aqueous media at constant ionic strength (1.00 M with CF_3SO_3Li). Observed pseudo-first-order rate constants (k_{obs}) and reaction conditions are given in Table 9. The temperature-dependent k_{obs} data from which the activation parameters were derived are contained in the supplementary material. A plot of $\ln(k/T)$ vs $1/T$ is linear. Values for ΔH^* and ΔS^* are obtained from a nonlinear least-squares fit of the data to the Eyring equation, which yields $\Delta H^* = 61.8(5)$ kJ mol^{-1} and $\Delta S^* = -81.9(1.6)$ J mol^{-1} K^{-1} at pH 2.84 and $[SCN^-] = 0.002$ M.

Table 6. Selected Bond Lengths (Å) and Angles (deg) for $[Re(terpy)_2C\ell](PF_6)_2$

Re–Cℓ	2.281(5)	N3–C15	1.35(2)
Re–N1	2.108(9)	N4–C16	1.36(2)
Re–N2	2.040(9)	N4–C20	1.36(2)
Re–N3	2.148(9)	N5–C21	1.38(2)
Re–N4	2.08(1)	N5–C25	1.35(2)
Re–N5	2.07(1)	N6–C26	1.39(2)
Re–N6	2.18(1)	N6–C30	1.31(2)
N1–C1	1.35(2)	C5–C6	1.44(2)
N1–C5	1.38(2)	C10–C11	1.44(2)
N2–C6	1.35(1)	C20–C21	1.44(2)
N2–C10	1.40(2)	C25–C26	1.41(2)
N3–C11	1.37(2)		
N1–Re–Cℓ	140.9(3)	N6–Re–N2	104.8(4)
N2–Re–Cℓ	89.2(3)	N6–Re–N3	150.2(4)
N2–Re–N1	73.4(4)	N6–Re–N4	129.2(4)
N3–Re–Cℓ	75.1(3)	N6–Re–N5	72.6(4)
N3–Re–N1	129.0(4)	C1–N1–Re	122.7(8)
N3–Re–N2	73.2(4)	C5–N1–Re	116.6(8)
N4–Re–Cℓ	140.3(3)	C6–N2–Re	121.8(8)
N4–Re–N1	78.8(4)	C10–N2–Re	119.2(8)
N4–Re–N2	109.1(4)	C11–N3–Re	115.3(8)
N4–Re–N3	77.1(4)	C15–N3–Re	125.8(9)
N5–Re–Cℓ	88.5(3)	C16–N4–Re	123.3(9)
N5–Re–N1	107.2(4)	C20–N4–Re	119.4(8)
N5–Re–N2	176.9(4)	C21–N5–Re	119.2(9)
N5–Re–N3	108.2(4)	C25–N5–Re	120.9(9)
N5–Re–N4	73.9(4)	C26–N6–Re	113.1(8)
N6–Re–Cℓ	75.1(3)	C30–N6–Re	124.4(9)
N6–Re–N1	75.9(4)		

Proton NMR. For all three reported $[Re(terpy)_2X]^{2+}$ complexes, unambiguous assignments of the proton resonances can be made from their chemical shifts, relative multiplicities, and integrated intensities, as well as from two-dimensional homonuclear shift correlation experiments[15] (Table 10). The free terpyridine ligand shows six proton signals since a symmetry plane passes through the nitrogen atom and carbon atom of the central pyridine ring. A detailed discussion of the ^1H NMR of free terpyridine was recently published.[8a] The internal symmetry of free terpy is not maintained in $[Re(terpy)_2X]^{2+}$ complexes since complexation causes the two terminal terpy rings to be nonequivalent. However, these $[Re(terpy)_2X]^{2+}$ complexes contain a 2-fold symmetry axis which passes through the Re–X bond and divides the complex into superimposable halves, each half containing a complete terpy ligand. As a result of these contrasting symmetry elements, the two coordinated terpy ligands are equivalent, but asymmetric; this results in 11 sharp signals in the aromatic proton region. A further proton signal is produced by the hydroxo ligand in $[Re(terpy)_2OH]^{2+}$. The terpyridine aromatic protons are designated by the following scheme:

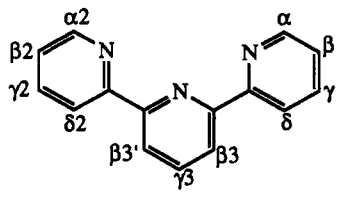

Discussion

Synthesis. Because ligand substitution onto $[Re^VOL_4]^n$ or $[Re^VO_2L_4]^n$ complexes is the usual mode of synthesis for new Re(V) complexes, it was expected that refluxing $[ReO_2(py)_4]^+$ with terpy might yield the Re(V) complex $[ReO_2(terpy)(py)]^+$. However, this Re(V) product is not observed; instead, 7-coordinate Re(III)–bis(terpyridine)-X complexes are produced by a reduction/substitution reaction. Reduction of the Re(V) starting material requires the contemporary oxidation of another species.

(15) Peters, W.; Fuchs, M.; Sicius, H.; Kuchen, W. *Angew. Chem., Int. Ed. Engl.* **1985**, *24*, 231–33.

Table 7. Fractional Atomic Coordinates for $[Re(terpy)_2NCS](SCN)_2 \cdot {}^1/_2H_2O$

atom	*x*	*y*	*z*
Re	0.35686(4)	0.21960(3)	0.27359(2)
N1	0.5651(7)	0.2224(5)	0.2446(5)
N2	0.4354(7)	0.1905(6)	0.3928(4)
N3	0.1892(7)	0.3094(6)	0.3795(4)
N4	0.3359(8)	0.4094(6)	0.2470(5)
N5	0.2671(7)	0.2527(6)	0.1606(4)
N6	0.4492(7)	0.0578(6)	0.1825(5)
C1	0.625(1)	0.253(1)	0.1604(7)
C2	0.770(1)	0.238(1)	0.1398(9)
C3	0.853(1)	0.194(1)	0.202(1)
C4	0.793(1)	0.171(1)	0.2841(8)
C5	0.6500(9)	0.1866(8)	0.3016(6)
C6	0.5753(9)	0.1651(8)	0.3915(6)
C7	0.630(1)	0.1362(9)	0.4701(8)
C8	0.539(1)	0.1391(9)	0.5495(7)
C9	0.395(1)	0.1782(8)	0.5521(6)
C10	0.3463(9)	0.2067(8)	0.4726(6)
C11	0.2021(9)	0.2689(7)	0.4639(6)
C12	0.089(1)	0.2856(8)	0.5324(6)
C13	−0.040(1)	0.3438(9)	0.5153(7)
C14	−0.0549(9)	0.3879(9)	0.4307(7)
C15	0.0618(9)	0.3674(8)	0.3641(6)
C16	0.388(1)	0.4842(9)	0.2930(7)
C17	0.347(1)	0.615(1)	0.2843(8)
C18	0.255(1)	0.6647(9)	0.2286(8)
C19	0.204(1)	0.5884(9)	0.1809(7)
C20	0.246(1)	0.4611(8)	0.1906(6)
C21	0.209(1)	0.3699(8)	0.1391(7)
C22	0.132(1)	0.390(1)	0.0703(7)
C23	0.120(1)	0.290(1)	0.0210(8)
C24	0.190(1)	0.171(1)	0.0373(7)
C25	0.2677(9)	0.1535(8)	0.1063(6)
C26	0.3667(8)	0.0410(8)	0.1233(6)
C27	0.385(1)	−0.0741(9)	0.0816(7)
C28	0.490(1)	−0.1729(9)	0.1006(7)
C29	0.572(1)	−0.1553(9)	0.1593(8)
C30	0.5512(9)	−0.0408(8)	0.1991(7)
S1	0.0841(3)	−0.0642(3)	0.3842(2)
C31	0.1784(8)	0.0246(8)	0.3434(5)
N7	0.2489(8)	0.0898(7)	0.3139(5)
S2	−0.0210(4)	0.0976(3)	0.8885(2)
C32	0.074(1)	0.1451(9)	0.8056(7)
N8	0.143(1)	0.180(1)	0.7475(7)
S3	0.50000	0.50000	0.00000
C33	0.629(3)	0.506(2)	0.060(2)
N9	0.707(3)	0.522(2)	0.103(2)
S4	0.553(1)	0.490(1)	0.4890(6)
C34	0.430(3)	0.475(3)	0.570(3)
N10	0.344(3)	0.467(3)	0.632(2)
O1	0.131(1)	0.455(1)	0.768(1)

The presence of ReO_4^- in the product mixture, combined with the overall low yield of these reactions, indicates disproportionation of Re(V) to Re(III) and Re(VII) (although oxidation of Re(V) to perrhenate by atmospheric oxygen, combined with reduction of Re(V) to Re(III) by ethanol, cannot be excluded *a priori*). A disproportionation mechanism can also be invoked for the production of the related $[Re^{II}(bpy)_3](ReO_4)_2$ complex from the reaction of $K_2[Re^{IV}F_6]$ with bpy in hot water at 85 °C;[16] low yields (30%) are also reported for this reaction. The stoichiometry generated by the proposed disproportionation is as follows:

$$4[Re^VO_2(py)_4]CF_3SO_3 + 4terpy + 2H_2O \rightarrow [Re^{III}(terpy)_2OH](Re^{VII}O_4)_2 + [Re^{III}(terpy)_2OH](CF_3SO_3)_2 + 2CF_3SO_3H + 16py$$

Thus, the theoretical yield of the insoluble $[Re^{III}(terpy)_2OH](ReO_4)_2$ is only 25% (based on total Re), in good agreement with the observed yield. This disproportionation stoichiometry also explains the fact that it is possible to increase the observed reaction yield by adding further NH_4ReO_4 to precipitate the rest of the Re(III) dication.

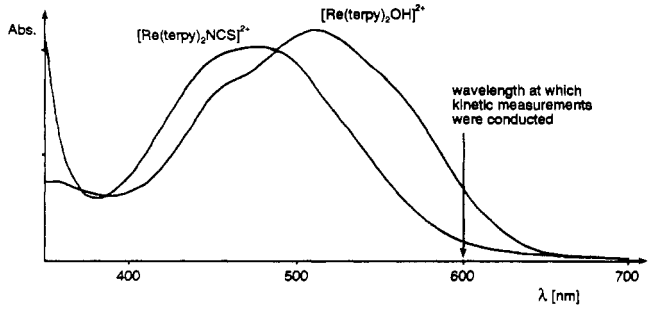

Figure 4. Electronic absorption spectrum of $[Re(terpy)_2OH]^{2+}$ contrasted with that of $[Re(terpy)_2NCS]^{2+}$.

Table 8. Selected Bond Lengths (Å) and Angles (deg) for $[Re(terpy)_2NCS](SCN)_2 \cdot {}^1/_2H_2O$

Re–N1	2.074(7)	N4–C16	1.34(1)
Re–N2	2.083(8)	N4–C20	1.37(1)
Re–N3	2.157(7)	N5–C21	1.35(1)
Re–N4	2.111(9)	N5–C25	1.38(1)
Re–N5	2.058(8)	N6–C26	1.37(1)
Re–N6	2.180(8)	N6–C30	1.36(1)
Re–N7	2.046(9)	C5–C6	1.49(2)
N1–C1	1.39(1)	C10–C11	1.47(1)
N1–C5	1.31(1)	C20–C21	1.44(2)
N2–C6	1.36(1)	C25–C26	1.44(1)
N2–C10	1.36(1)	S1–C31	1.59(1)
N3–C11	1.37(1)	C31–N7	1.17(1)
N3–C15	1.34(1)		
Re–N1–C1	121.6(6)	N1–Re–N6	77.3(3)
Re–N1–C5	122.2(7)	N1–Re–N7	136.0(3)
Re–N2–C6	120.3(7)	N2–Re–N3	73.6(3)
Re–N2–C10	119.8(6)	N2–Re–N4	106.3(3)
Re–N3–C11	115.5(6)	N2–Re–N5	176.4(3)
Re–N3–C15	122.5(7)	N2–Re–N6	109.5(3)
Re–N4–C16	123.0(7)	N2–Re–N7	86.8(3)
Re–N4–C20	117.1(7)	N3–Re–N4	78.0(3)
Re–N5–C21	120.9(7)	N3–Re–N5	102.9(3)
Re–N5–C25	119.1(6)	N3–Re–N6	147.1(3)
Re–N6–C26	113.7(6)	N3–Re–N7	73.9(3)
Re–N6–C30	124.2(7)	N4–Re–N5	73.2(3)
Re–N7–C31	173.1(8)	N4–Re–N6	128.8(3)
N1–Re–N2	72.7(3)	N4–Re–N7	144.1(3)
N1–Re–N3	132.0(3)	N5–Re–N6	73.1(3)
N1–Re–N4	79.8(3)	N5–Re–N7	91.7(3)
N1–Re–N5	110.6(3)	N6–Re–N7	73.5(3)
		S1–C31–N7	179.3(9)

Table 9. Selected Observed Pseudo-First-Order Rate Constants for the Formation of $[Re(terpy)_2NCS]^{2+}$ from $[Re(terpy)_2OH^{2+}$ [a]

$[NCS^-]$, M	pH	$[H^+]$, M	buffer	k_{obs}, s^{-1}
0.003	2.40	4.0×10^{-3}	none	$1.74(1) \times 10^{-2}$
0.012	2.40	4.0×10^{-3}	none	$6.67(14) \times 10^{-2}$
0.024	2.42	3.8×10^{-3}	none	$1.21(1) \times 10^{-1}$
0.10	5.96	1.1×10^{-6}	MES	$2.85(1) \times 10^{-4}$
0.40	5.95	1.2×10^{-6}	MES	$9.96(1) \times 10^{-4}$
0.80	5.93	1.2×10^{-6}	MES	$1.461(4) \times 10^{-3}$
0.002	2.70	0.0020	none	$6.91(3) \times 10^{-3}$
0.002	2.04	0.0091	none	$2.14(2) \times 10^{-2}$
0.002	1.51	0.0309	none	$4.29(4) \times 10^{-2}$
0.002	1.02	0.0955	none	$6.29(9) \times 10^{-2}$
0.002	0.83	0.1479	none	$6.3(6) \times 10^{-2}$
0.002	0.62	0.2399	none	$7.4(6) \times 10^{-2}$
0.8	8.95	1.1×10^{-9}	TAPS	$3.9(1) \times 10^{-5}$
0.8	8.06	8.7×10^{-9}	TAPS	$6.7(1) \times 10^{-5}$
0.8	7.39	4.1×10^{-8}	BES	$1.12(1) \times 10^{-4}$
0.8	6.34	4.6×10^{-7}	MES	$5.98(1) \times 10^{-4}$
0.8	5.51	3.1×10^{-6}	MES	$3.53(1) \times 10^{-3}$

[a] $[Re(terpy)_2OH]^{2+}$ initial concentration 1.66×10^{-4} M; $\mu = 1.00$ M ($LiCF_3SO_3$); $T = 25$ °C.

The course of the synthetic reaction is affected by reaction time, reaction temperature, and solvent. In ethanol/water mixtures, complete reaction is obtained only after 18 h of refluxing. Reaction in absolute ethanol yields the desired Re(III) products, but they are always contaminated by ReO_2. Reaction in pure water does not yield the 7-coordinate Re(III) products, but rather generates a pale pink solution which, from its simple, six-line, ^1H NMR spectrum, may contain the Re(I) species $[Re(terpy)_2]^+$. The course of the synthetic reaction is also strongly affected by the choice of starting material. The identity of any monodentate ligand introduced with the Re(V) starting material (*e.g.*, as a counterion) is especially important in that it often determines the identity of the monodentate (*i.e.*, the seventh) ligand in the Re(III) product. When the starting material is *trans*-$[ReO_2(py)_4]CF_3SO_3$, pure $[Re(terpy)_2OH]^{2+}$ complex is formed. When the starting material is *trans*-$[ReO_2(py)_4]Cl$, a mixture of $[Re(terpy)_2OH]^{2+}$ and $[Re(terpy)_2Cl]^{2+}$ products is formed. Even the addition of excess NH_4Cl to increase the concentration of chloride ions in the reaction mixture does not allow the recovery of pure $[Re(terpy)_2Cl]^{2+}$, either in solution or in the solid state. A more successful approach involves acidification of the solution containing $[Re(terpy)_2OH]^{2+}$, or a $[Re(terpy)_2OH]^{2+}/[Re(terpy)_2Cl]^{2+}$ mixture, with HCl followed by precipitation with a concentrated aqueous NH_4ReO_4 solution. This acid-catalyzed substitution proved to be the most useful route for conversion of $[Re(terpy)_2OH]^{2+}$ into other $[Re(terpy)_2X]^{2+}$ species. Thus, $[Re(terpy)_2OH]^{2+}$ in acetonitrile or water can be completely converted into the corresponding $[Re(terpy)_2NCS]^{2+}$ species by reaction with a large excess of KSCN and CF_3SO_3H.

Crystallography. The terpyridine ligand is physically suited to higher coordination numbers.[17,18] Its ~70° bite angle is near the calculated L–M–L angle for some positions in all three idealized 7-coordinate polyhedra. However these three structures comprise the first reported bis(terpyridine)–metal complexes with expanded coordination numbers; all others have been octahedral and 6-coordinate. Both Re(III) and Tc(III) can be 6- or 7-coordinate. Hexacoordination is normal for "ionic" complexes (*i.e.*, those containing σ-donor ligands) and provides 16 electrons for Tc(III) and Re(III) centers. However, heptacoordination yields an 18-electron, filled-shell configuration which seems to be preferred for "covalent" complexes (*i.e.*, those which contain π-back-bonding ligands). For example, many of the reported 7-coordinate Re(III) complexes contain isocyanide ligands; these result from the interest in reductive coupling of linear ligands in high coordinate complexes.[19] Other well-characterized rhenium(III) heptacoordinate complexes contain either phosphine, dithiolate or carbonyl ligands.[20] Polypyridyl ligands, such as terpy, are capable π-back-bonders. Upon close examination, the terpy arrangement in $[Re(terpy)_2X]^{2+}$ is only a small twist away from providing an octahedral coordination environment. It is easy to imagine release of the seventh X^- ligand followed by a facial twist to convert the trigonal prism into an octahedral coordination environment. The syntheses described above imply facile substitution of the seventh, monodentate, ligand, perhaps even

(16) Stebler, M.; Gutièrrez, A.; Ludi, A.; Bürgi, H.-B. *Inorg. Chem.* **1987**, *26*, 1449–51.
(17) (a) Wieghardt, K.; Holzbach, W.; Weiss, J. *Z. Naturforsch.* **1982**, *37B*, 680–3. (b) Beck, J.; Strähle, J. *Z. Naturforsch.* **1985**, *40B*, 891–4. (c) Beck, J.; Schweda, E. Strähle, J. *Z. Naturforsch.* **1985**, *40b*, 1073–6. (d) Beck, J.; Strähle, J. *Z. Anorg. Allg. Chem.* **1987**, *554*, 50–60.
(18) Al-Ani, F. T.; Hughes, D. L.; Pickett, C. J. *J. Chem. Soc., Dalton Trans.* **1988**, 1705–7.
(19) (a) Warner, S.; Lippard, S. J. *Inorg. Chem.* **1989**, *28*, 3008–13. (b) Treichel, P. M.; Williams, J. P.; Freeman, W. A.; Gelder, J. I. *J. Organomet. Chem.* **1979**, *170*, 247–58. (c) Farr, J. P.; Abrams, M. J.; Costello, C. E.; Davison, A.; Lippard, S. J. *Organometallics* **1985**, *4*, 139–42. (d) Warner, S.; Cheatham, L. K.; Tulip, T. H.; Williams, I. D.; Lippard S. J. *Inorg. Chem.* **1991**, *30*, 1221–6. (e) Kiernan, P. M.; Griffith, W. P. *Inorg. Nucl. Chem. Lett.* **1976**, *12*, 377–80. (f) Freni, M.; Romiti, P. *J.Organomet Chem.* **1975**, *87*, 241–5.
(20) (a) Drew, M. G. B.; Davis, K. M.; Edwards, D. A.; Marshalsea, J.; *J. Chem. Soc., Dalton Trans.* **1978**, 1098–102. (b) Moehring, G. A.; Walton, R. A. *J. Chem. Soc., Dalton Trans.* **1987**, 715–20. (c) Fletcher, S. R.; Skapski, A. C. *J. Chem. Soc., Dalton Trans.* **1974**, 486–9. (d) Ichimura, A.; Yamamoto, Y.; Kajino, T.; Kitagawa, T.; Kuma, H.; Kushi, Y. *J. Chem. Soc., Chem. Commun.* **1988**, 1130–1. (e) A related Tc(III) example is given in: Nicholson, T.; Thornback, J.; O'Connell, L.; Morgan, G.; Davison, A.; Jones, A. G. *Inorg. Chem.* **1990**, *29*, 89–92.

Table 10. ^{1}H NMR Data for $[Re(terpy)_2X]^{2+}$ in Acetonitrile

	δ, ppm				coupling, Hz	
proton	X = OH	X = Cl	X = NCS	multiplicity[a]	X = OH, X = Cl, X = NCS	rel integ
H_α	6.70	6.91	7.00	d	$^3J(H_\alpha H_\beta)$ = 5.8, 5.8, 5.6	2 H
H_β	6.95	7.08	7.17	m		2 H
H_γ	7.97	8.07	8.14	t	$^3J(H_\gamma H_\delta = H_\gamma H_\beta)$ = 7.8, 8.0, 8.0	2 H
H_δ	8.64	8.62	8.70	d	$^3J(H_\delta H_\gamma)$ = 7.8, 8.0, 8.0	2 H
$H_{\alpha 2}$	7.54	7.43	7.50	d	$^3J(H_{\alpha 2} H_{\beta 2})$ = 5.9, 5.8, 5.7	2 H
$H_{\beta 2}$	6.92	6.97	7.02	m		2 H
$H_{\gamma 2}$	8.02	8.10	8.15	t	$^3J(H_{\gamma 2} H_{\delta 2} = H_{\gamma 2} H_{\beta 2})$ = 7.7, 8.1, 8.1	2 H
$H_{\delta 2}$	9.06	9.08	9.12	d	$^3J(H_{\delta 2} H_{\gamma 2})$ = 7.7, 8.1, 8.1	2 H
$H_{\beta 3}$	9.03	9.07	9.07	d	$^3J(H_{\beta 3} H_{\gamma 3})$ = 7.9, 8.0, 8.0	2 H
$H_{\beta 3'}$	9.25	9.31	9.33	d	$^3J(H_{\beta 3'} H_{\gamma 3})$ = 7.9, 8.0, 8.0	2 H
$H_{\gamma 3}$	8.17	8.28	8.29	t	$^3J(H_{\gamma 3} H_{\beta 3} = H_{\gamma 3} H_{\beta 3'})$ = 7.9, 8.0, 8.0	2 H
O*H*	4.49			s		1 H

[a] s = singlet; d = doublet; t = triplet; m = multiplet.

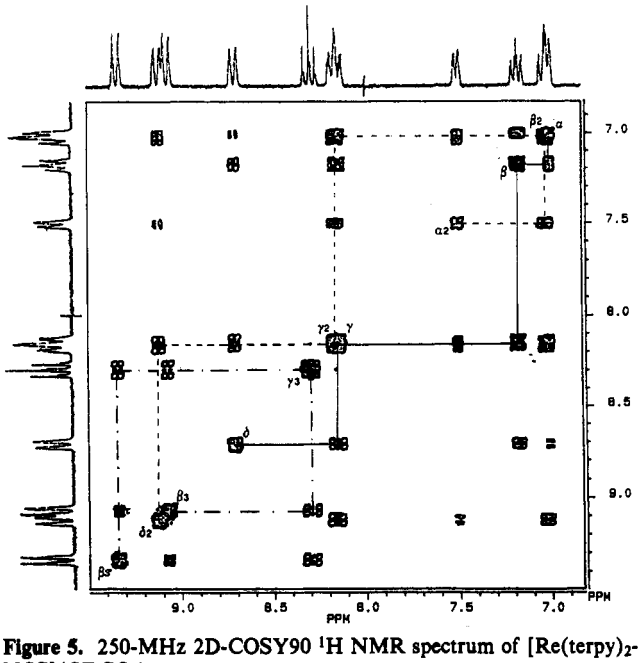

Figure 5. 250-MHz 2D-COSY90 ^{1}H NMR spectrum of $[Re(terpy)_2NCS](CF_3SO_3)_2$.

equilibrium distributions of 6- and 7-coordinate species. The stable 7-coordinate species reported herein may be excellent models for the activated complex generated during associative substitution reactions of octahedral complexes.

The sole other Re–terpyridine complex known to us, in which the terpy is tridentate, was only recently structurally characterized.[8a] This 6-coordinate $[ReO(terpy)(SC_6H_4CH_3)_2]^+$ complex contains the $(Re^V{=}O)^{3+}$ core which is isoelectronic with Re^{3+} and generally exhibits similar M–L distances.[8,21,22] The terpy ligand in $[ReO(terpy)(SC_6H_4CH_3)_2]^+$ is more planar than the terpy ligands in the $[Re(terpy)_2X]^{2+}$ complexes, which is not surprising in light of the increased steric pressure imposed by 7-coordination. But, otherwise, similar Re–N distances and N–Re–N bite angles are observed (*viz.* Re^V–N = 2.09(1) Å (distal), Re^V–N = 2.187(6) Å (central), but subject to an oxo *trans* effect), and the terpy bite angles are 73(1)° in $[ReO(terpy)(SC_6H_4CH_3)_2]^+$. There is also only one Tc-terpyridine complex known to us:[23] $[TcBr(PMe_2Ph)_2(terpy)]^+$. In this Tc(II) complex, the Tc-N(terpy) bond lengths are 2.00 Å (central) and 2.10 Å (distal), which are only slightly shorter than those observed for Re(III) herein.

Re–OH and Tc–OH examples in structural determinations are relatively rare. No Re^{III}–OH structures are published. There are occasional examples of bridging μ-OH groups in Re and Tc complexes, but very few monomeric complexes of Re or Tc with hydroxo ligands are available for comparison. Of these, $[Re^{IV}Cl_3(PEt_2Ph)_2(OH)]$ exhibits a very short Re–OH length (1.795 Å); this short length and the IR spectrum of the complex raise questions about the bond type.[24] The structure of $[Re^V(en)_2(O)(OH)]^{2+}$ has been reported in an abstract but no details have been forthcoming.[25] The remaining two examples $[Re^V(CN)_4(O)(OH)]^{2-}$ [26] and $[Tc^V(DMPE)_2(O)(OH)]^{2+}$ [27] both contain hydroxo groups *trans* to the strong electron donating oxo group; Re^V–OH = 1.902 Å and Tc^V–OH = 1.96 Å (from EXAFS analysis). Therefore, the reported structure of $[Re(terpy)_2OH]^{2+}$ is useful in that it describes a bond type which until now has been ill-defined.

There are many examples of Re–Cl bonds for comparison. The most useful are those Re^{III}–Cl bonds that are *trans* to other Cl ligands; in these cases, the Re^{III}–Cl length is ~2.33 Å.[19a,28] Longer Re^{III}–Cl bond distances often occur with other *trans* ligands (*ca.* 2.37–2.47 Å).[29] In another report, three 6-coordinate Re^{III} complexes containing Cl with ammine or pyridine coligands showed an average Re^{III}–Cl distance of 2.35(1) Å.[30] It is noteworthy that, in $[Re^{III}(terpy)_2Cl]^{2+}$, the Re^{III}–Cl length is 2.281(5) Å, which is definitely shorter than what would have been predicted, especially since the environment is 7-coordinate. This implies the presence of considerable π-back-bonding between Re and terpy.

Re^{III}–NCS bonds have been examined both in dimeric complexes (containing a metal–metal bond) such as $[Re_2(NCS)_8 \cdot 2(CH_3)_2CO]^{2-}$ [31] (Re–N = 2.003(8) Å) and $[Re_2(NCS)_8 \cdot 2C_5H_5N]^{2-}$ [31] (Re–N = 1.995(9) Å) and in the monomeric complex $[Re^{III}(NCS)_3(PEt_2Ph)(DPPE)]$ (Re–N = 2.00(1) Å *trans* to NCS and 2.061 Å *trans* to phosphine).[32] In the light of these results, the Re^{III}–NCS length in $[Re^{III}(terpy)_2NCS]^{2+}$ seems somewhat long at 2.046(9) Å. However, the hexakis(isothio-

(21) Konno, T.; Heeg, M. J.; Deutsch, E. *Inorg. Chem.* **1988**, *27*, 4113–21.
(22) Chen, B.; Heeg, M. J.; Deutsch, E. *Inorg. Chem.* **1992**, *31*, 4683–90.
(23) Wilcox, B. E.; Ho, D. M.; Deutsch, E. *Inorg. Chem.* **1989**, *28*, 3917–23.
(24) Sacerdoti, M.; Bertolasi, V.; Gilli, G.; Duatti, A. *Acta Crystallogr.* **1982**, *B38*, 96–100.
(25) Betzner, G. L.; Che'ng, W.; Jayadevan, N. C.; Lock, C. J. L.; Brown, I. D. *Acta Crystallogr.* **1966**, *A136*, 21.
(26) Purcell, W.; Roodt, A.; Basson, S. S.; Leipoldt, J. G. *Transition Metal Chem. (London)* **1989**, *14*, 224–6.
(27) Vanderheyden, J.-L.; Ketring, A. R.; Libson, K.; Heeg, M. J.; Roecker, L.; Motz, P.; Whittle, R.; Elder, R. C.; Deutsch, E. *Inorg. Chem.* **1984**, *23*, 3184–91.
(28) Vanderheyden, J.-L.; Heeg, M. J.; Deutsch, E. *Inorg. Chem.* **1985**, *24*, 1666–73.
(29) (a) Ferretti, V.; Sacerdoti, M.; Bertolasi, V.; Rossi, R. *Acta Crystallogr.* **1984**, *40*, 974–6. (b) Rossi, R.; Duatti, A.; Magon, L; Casellato, U.; Graziani, R.; Toniolo, L. *J. Chem. Soc., Dalton Trans.* **1982**, 1949–52. (c) Duckworth, V. F.; Douglas, P. G.; Mason, R.; Shaw, B. L. *J. Chem. Soc. D* **1970**, 1083–4. (d) Mason, R.; Thomas, K. M.; Zubieta, J. A.; Douglas, P. G.; Galbraith, A. R.; Shaw, B. L. *J. Am. Chem. Soc.* **1974**, *96*, 260–2. (e) Brown, I. D.; Lock, C. J. L.; Wan, C. *Can. J. Chem.* **1974**, *52*, 1704–8.
(30) Orth, S. D.; Barrera, J.; Sabat, M.; Harman, W. D. *Inorg. Chem.* **1993**, *32*, 594–601.
(31) Cotton, F. A.; Matusz, M. *Inorg. Chem.* **1987**, *26*, 3468–72.
(32) Hahn, J. E.; Nimry, T.; Robinson, W. R.; Salmon, D. J.; Walton, R. A. *J. Chem. Soc., Dalton Trans.* **1978**, 844–8.

cyanato)technetium(III) complex[33] exhibits a Tc^{III}–N length of 2.049 Å, in agreement with the Re^{III}–N length reported herein. A survey of the Cambridge Crystallographic Database[34] for all rhenium and technetium complexes containing NCS ligands shows that in every case the mode of bonding is through the nitrogen.

^{1}H NMR Spectra. The 7-coordinate $[Re(terpy)_2X]^{2+}$ complexes contain a Re(III) metal center with a d^4 electronic configuration in a distorted capped trigonal prism environment (*vide infra*). In this environment two of the three t_{2g} d orbitals (d_{xy} and d_{yz}) are sufficiently lowered in energy[35] to result in a diamagnetic material which exhibits sharp and distinct proton resonances. Table 10 presents the chemical shift values, spin–spin splitting patterns, coupling constants, and relative integrations for all three Re(III) complexes. The complexes contain two equivalent but asymmetric terpy ligands; this results in 11 proton signals in the aromatic region.

Assignments of the resonances of the central terpy ring are quite direct. 2D-COSY experiments provide clear evidence for an ABB′ system and its relative couplings (*e.g.* Figure 5). The signals which arise from the two terminal terpy rings are more complicated to assign; these are comprised of two ABCD proton systems, again distinguishable by means of the two-dimensional map. But, for a complete assignment, two questions need to be resolved: (i) Which is the α proton since it is likely to be confused with the δ one, and (ii) which set of protons belong to one terminal ring and which to the other? In consideration of the first question, we note that the coupling constant between α and β protons in related N-aromatic systems is smaller than the corresponding $^3J(H_\delta H_\gamma)$.[36] Moreover, in a recent publication, α protons of similar N-aromatic bipyridine and phenanthroline ligands coordinated to a Tc(III) center are reported to be the highest upfield protons with respect to the other aromatic ones.[37] These two observations allow us to assign within the ABCD system the most downfield doublet as δ and the most upfield as α proton signals. With respect to the second question raised above, the two terminal rings on each terpy ligand can be distinguished only by changing the seventh X coordinating ligand. Replacement of the hydroxo ligand by chloride or isothiocyanate causes an appreciable downfield shift only of the α proton signal of the rings opposite the Re–X bond (associated with N1 and N4) while the shifts of the other ring protons remain almost unaffected. Increasing the π-back-bonding capability of the X group from OH to Cl to NCS provides better delocalization of negative charge density and consequently a downfield shift of the α protons nearest N1 and N4. The α protons of the N3 and N6 rings are much less affected by varying X.

An interesting comparison can be made with the proton NMR data for hexacoordinate bis(terpyridine)–Ru(II) complexes.[38] In these complexes, the chemical shift changes, induced upon complexation, for two protons of the terpy ligand (H_α and $H_{\gamma 3}$ in our labeling) are reported to be diagnostic for their chemical environment. Even though the geometry of these octahedral ruthenium complexes differs from that of our 7-coordinated $[Re(terpy)_2X]^{2+}$ complexes, several spectroscopic analogies are observed. For example, relative to those of the free terpy molecule, H_α protons in $[Ru(terpy)_2]^{2+}$ are shifted upfield 1.36 ppm while the $H_{\gamma 3}$ protons are shifted downfield 0.46 ppm. These values are in acceptable agreement with those found for $[Re(terpy)_2X]^{2+}$ complexes. In both these ruthenium(II) and rhenium(III) complexes, the $H_{\gamma 3}$ protons of the central pyridine ring are held out of any shielding plane determined by the two distal pyridine rings and consequently they are shifted downfield. On the contrary, the H_α protons are held somewhat over the shielding plane of the central pyridine rings. Where only π-terpyridine ring shielding is active, the upfield shift is around 1.20 ppm ($H_{\alpha 2}$). Where the π-terpyridine ring shielding is active along with greater electronic overlap dictated by symmetry considerations (as in the py ring "*trans*" to the Re–X linkage) the upfield shift is increased to an average of 1.80 ppm (H_α).

Electronic Spectra. Table 2 summarizes the electronic absorption data for the $[Re(terpy)_2X]^{2+}$ complexes. The spectra consist of two well-defined regions. Relatively intense absorptions generally composed of two distinct bands are observed in the region 290–330 nm (this region is obscured for $[Re(terpy)_2NCS]^{2+}$ in water by the presence of KSCN). These absorptions are attributed to π–π^* transitions associated with the aromatic rings of the terpy ligands themselves.

A less intense, longer wavelength band around 500 nm is assigned to a metal-to-terpy charge transfer (CT) transition, similar to that observed in $[Ru^{II}(terpy)_2]^{2+}$.[38] The energy of this band is somewhat dependent on the nature of X in $[Re(terpy)_2X]^{2+}$ complexes: as expected from its assignment as a metal-to-terpy CT transition, the position moves from 512 nm when X is the electron donating OH to 478 nm when X is the stronger π-accepting ligand NCS. This difference in spectra allows the kinetics of conversion of the OH complex to the NCS complex to be monitored spectrophotometrically (see Figure 4). In water, protonation of the hydroxo complex shifts the position of this band from 512 to 486 nm. This protonation is an important aspect of the chemistry of $[(terpy)_2ReOH]^{2+}$ since the protonated complex undergoes substitution much more rapidly than does the hydroxy complex (*vide infra*).

Kinetics and Mechanism. The monitored reaction is as follows:

$$[Re(terpy)_2OH]^{2+} + NCS^- \rightarrow [Re(terpy)_2NCS]^{2+} + OH^-$$

In the presence of large excesses of NCS^-, the hydroxo complex disappears in a first-order fashion. The pseudo first-order rate constant k_{obs} is linearly dependent on the concentration of thiocyanate. This is true at low pH values, where the reaction is fast, and at higher pH values, where the reaction is very slow. A small intercept is observed in the plots of k_{obs} vs [SCN^-]. Possible explanations for this are (a) the presence of a second, [SCN^-]-independent, pathway, (b) a medium effect, or (c) a contribution from the back-reaction ($[Re(terpy)_2NCS]^{2+} \rightarrow [Re(terpy)_2OH]^{2+}$).[39] Because the intercept is statistically not well defined (the esd is about 20%–50%), its mechanistic significance is correspondingly uncertain.

Due to the protonation of $[Re(terpy)_2OH]^{2+}$ (*vide supra*), the concentration of hydrogen ion greatly affects the observed rate constants. The acid dependence of k_{obs} is consistent with a mechanism in which $[Re(terpy)_2OH]^{2+}$ participates in a rapid protonation equilibrium prior to rate-determining ligand substitution. A plot of k_{obs} vs pH from pH 0.6 to 2.7 qualitatively suggests an approximate pK_a value for the protonated complex of 1.5 (supplementary figure). No statistically defined intercept is found in a plot of k_{obs} vs [H^+], and thus an acid independent pathway corresponding to direct reaction of SCN^- with the hydroxy complex does not appear to be significant.

(33) Trop, H. S.; Davison, A.; Jones, A. G.; Davis, M. A.; Szalda, D. J.; Lippard, S. J. *Inorg. Chem.* **1980**, *19*, 1105–10.
(34) Cambridge Crystallographic Database: Allen, F. H.; Kennard, O.; Taylor, R. *Acc. Chem. Res.* **1983**, *16*, 146–53.
(35) Huheey, J. E. *Inorganic Chemistry*, 3rd ed.; Harper and Row: New York, 1983; p 412.
(36) The free-typridine proton NMR spectrum in CD_3CN shows H_α at 8.66 ppm, with $^3J(H_\alpha H_\beta)$ = 4.8 Hz and H_δ at 8.62 ppm with $^3J(H_\delta H_\gamma)$ = 7.8 Hz. Analogously, the free pyridine molecule in $CDNO_3$ exhibits $^3J(H_\alpha H_\beta)$ smaller than the coupling constants related to the other aromatic protons. When pyridine coordinates around Tc and Re metals, giving *trans*-dioxo $MO_2(py)_4^+$ species, such behavior is retained. See also: Tisato, F.; Refosco, F.; Moresco, A.; Bandoli, G.; Mazzi, U.; Nicolini, M. *J. Chem. Soc., Dalton Trans.* **1990**, 2225–32.
(37) Breikss, A. I.; Nicholson, T.; Jones, A. G.; Davison, A. *Inorg. Chem.* **1990**, *29*, 640–5.
(38) Thummel, R. P.; Jahng, Y. *Inorg. Chem.* **1986**, *25*, 2527–34.
(39) Frost, A. A.; Pearson, R. G. *Kinetics and Mechanism*, 2nd ed., Wiley and Sons: New York, 1953; p 186.

The following mechanism for the substitution of SCN^- onto $[Re(terpy)_2OH]^{2+}$ to form $[Re(terpy)_2NCS]^{2+}$ is consistent with all the kinetic and spectrophotometric data in hand:

$$[Re(terpy)_2OH]^{2+} + H^+ \overset{\text{fast, } K_a^{-1}}{\rightleftharpoons} [Re(terpy)_2OH_2]^{3+}$$

$$[Re(terpy)_2OH_2]^{3+} + SCN^- \underset{k_{-2}}{\overset{\text{slow, } k_2}{\rightleftharpoons}} [Re(terpy)_2NCS]^{2+} + H_2O$$

Where K_a is defined as

$$K_a = \frac{[[Re(terpy)_2OH]^{2+}][H^+]}{[[Re(terpy)_2OH_2]^{3+}]}$$

The rate law predicted by this mechanism is

$$k_{obs} = k_2[SCN^-]\frac{[H^+]}{[H^+] + K_a} + k_{-2}$$

A nonlinear least-squares fit to this expression of the rate constants (k_{obs}) obtained at various hydrogen ion concentrations with $[SCN^-] = 0.002$ M gives the following results:

$$k_2 = 45(4)\ M^{-1}\ s^{-1}$$

$$K_a = 0.045(16)\ M$$

$$k_{-2} = 1.1(1.4) \times 10^{-4}\ M^{-1}\ s^{-1}$$

The calculated value of k_{-2} is statistically undefined, confirming that the back-reaction does not play an important role under these conditions. However, this k_{-2} pathway must exist, since experimentally it has been shown that $[Re(terpy)_2NCS]^{2+}$ can be converted to $[Re(terpy)_2OH]^{2+}$ at higher pH values.

The kinetic data establish that the substitution of thiocyanate onto $[Re(terpy)_2OH]^{2+}$ to yield $[Re(terpy)_2NCS]^{2+}$ proceeds through a protonated form which is in equilibrium with the hydroxo complex. We have chosen above to formulate this protonated species as the 7-coordinate $[Re(terpy)_2OH_2]^{3+}$, although it could equally well be formulated as the 6-coordinate $[Re(terpy)_2]^{3+}$ which could be hypothesized to be in rapid equilibrium with the aquo complex:

$$[Re(terpy)_2OH]^{2+} + H^+ \rightleftharpoons [Re(terpy)_2OH_2]^{3+} \rightleftharpoons [Re(terpy)_2]^{3+} + H_2O$$

Reaction of the protonated form with NCS^- is first-order in thiocyanate. This result is easily understood if the protonated species is the 6-coordinate $[Re(terpy)_2]^{3+}$ but is difficult to understand if the protonated species is the 7-coordinate $[Re(terpy)_2OH_2]^{3+}$. Associative activation of the 7-coordinate $[Re(terpy)_2OH_2]^{3+}$ to yield an 8-coordinate reaction intermediate is unpalatable and unprecedented,[40] while a prior outer-sphere equilibrium involving SCN^- is unlikely to provide an effective reaction pathway. None of the results gathered in this preliminary kinetic investigation are able to distinguish among the several mechanistic possibilities, and so further NMR studies are planned to better characterize the solution chemistry of $[Re(terpy)_2OH]^{2+}$ and its protonated form.

Acknowledgment. Financial support was provided by National Institutes of Health Grants HL-21276 and CA-42179 (E.D.), by a CNR research grant (F.T.), and by the German Academic Exchange Service (F.W. and J.R.).

Supplementary Material Available: Figures A–F, showing kinetic data plots for the conversion of $[Re(terpy)_2OH]^{2+}$ to $[Re(terpy)_2NCS]^{2+}$, Tables A and B, listing kinetic data, Table C, presenting a comparison of proton chemical shifts of free terpyridine with those of complexed terpyridine, and Tables D–H, I–M, and N–R, containing supplemental crystallographic data, anisotropic thermal parameters, hydrogen parameters, bond lengths, and bond angles for $[Re(terpy)_2OH](PF_6)_2 \cdot H_2O$, $[Re(terpy)_2Cl](PF_6)_2$, and $[Re(terpy)_2NCS](SCN)_2 \cdot {}^1/_2H_2O$ (29 pages). Ordering information is given on any current masthead page.

(40) Lindmark, A. F. *Inorg. Chem.* **1992**, *31*, 3507–13.